

AD _____

Award Number: W81XVWH-12-1-0051

TITLE: **Activation of mTor Signaling by Gene Transduction to Induce Axon Regeneration in the Central Nervous System Following Neural Injury**

PRINCIPAL INVESTIGATOR: Robert E. Burke, MD

CONTRACTING ORGANIZATION:

COLUMBIA UNIVERSITY MEDICAL CENTER

NEW YORK NY 10032-3725

REPORT DATE: MARCH 2014

TYPE OF REPORT: FINAL

PREPARED FOR: U.S. Army Medical Research and Materiel Command
Fort Detrick, Maryland 21702-5012

DISTRIBUTION STATEMENT: Approved for Public Release;
Distribution Unlimited

The views, opinions and/or findings contained in this report are those of the author(s) and should not be construed as an official Department of the Army position, policy or decision unless so designated by other documentation.

REPORT DOCUMENTATION PAGE				Form Approved OMB No. 0704-0188	
Public reporting burden for this collection of information is estimated to average 1 hour per response, including the time for reviewing instructions, searching existing data sources, gathering and maintaining the data needed, and completing and reviewing this collection of information. Send comments regarding this burden estimate or any other aspect of this collection of information, including suggestions for reducing this burden to Department of Defense, Washington Headquarters Services, Directorate for Information Operations and Reports (0704-0188), 1215 Jefferson Davis Highway, Suite 1204, Arlington, VA 22202-4302. Respondents should be aware that notwithstanding any other provision of law, no person shall be subject to any penalty for failing to comply with a collection of information if it does not display a currently valid OMB control number. PLEASE DO NOT RETURN YOUR FORM TO THE ABOVE ADDRESS.					
1. REPORT DATE (DD-MM-YYYY) March 2014		2. REPORT TYPE FINAL		3. DATES COVERED (From - To) 21February2013-20February2014	
4. TITLE AND SUBTITLE Activation of mTor Signaling by Gene Transduction to Induce Axon Regeneration in the Central Nervous System Following Neural Injury				5a. CONTRACT NUMBER	
				5b. GRANT NUMBER W81XWH-12-1-0051	
				5c. PROGRAM ELEMENT NUMBER	
6. AUTHOR(S) Robert E. Burke, MD email:rb43@columbia.edu				5d. PROJECT NUMBER	
				5e. TASK NUMBER	
				5f. WORK UNIT NUMBER	
7. PERFORMING ORGANIZATION NAME(S) AND ADDRESS(ES) COLUMBIA UNIVERSITY MEDICAL CENTER NEW YORK NY 10032-3725				8. PERFORMING ORGANIZATION REPORT NUMBER	
9. SPONSORING / MONITORING AGENCY NAME(S) AND ADDRESS(ES) U.S. Army Medical Research and Materiel Command Fort Detrick, Maryland				10. SPONSOR/MONITOR'S ACRONYM(S)	
				11. SPONSOR/MONITOR'S REPORT NUMBER(S)	
12. DISTRIBUTION / AVAILABILITY STATEMENT Approved for Public Release; Distribution Unlimited					
13. SUPPLEMENTARY NOTES					
14. ABSTRACT A longstanding concept in neuroscience has been that the mature mammalian brain is incapable of axon regeneration. However, we have shown that it is possible to achieve long range axon growth by re-activation of intrinsic genetic programs that are active during development. We have found that activation of Akt/mTor signaling by AAV-mediated transduction with either the kinase Akt or the GTPase Rheb in a model of retrograde axonal degeneration induces axon growth by dopamine neurons. However, these molecules cannot be directly used in therapeutics because they are oncogenes. The goal of this proposal therefore is to develop a strategy to circumvent this problem. We have hypothesized that mediators downstream of mTor may diverge in their effects, making it possible to achieve axon growth without oncogenic risk. In Year 01 we had shown that one mTor target, p70S6K, is able to induce new axon growth. In Year 02 we have assessed the ability of a second mTor target, eIF4E, to induce new axon growth. We have found that transduction of dopamine neurons of the SN by AAV eIF4E at three weeks after axonal destruction with the neurotoxin 6OHDA does not induce new axon growth. This conclusion was reached by assessments based on three techniques: immunostaining for tyrosine hydroxylase-positive axons in the medial forebrain bundle (MFB); quantification by confocal optical dissection of either GFP-positive axons in the MFB in transgenic TH-GFP mice or of Tomato-positive axons following transduction with anterograde tracer Tomato-Tau. As anticipated, based on anatomical evidence showing an inability of AAV eIF4E to re-establish anatomical contact, we found no reversal of a toxin-induced behavioral deficit. We conclude that of the two mTor targets, p70S6K and eIF4E, only p70S6K is an effective mediator of new axon growth. It will therefore be the focus of a refined, axon-targeting strategy in Year 03 of this proposal.					
15. SUBJECT TERMS Axon regeneration, mTor, Akt, substantia nigra, gene therapy					
16. SECURITY CLASSIFICATION OF:			17. LIMITATION OF ABSTRACT UU	18. NUMBER OF PAGES 25	19a. NAME OF RESPONSIBLE PERSON USAMRMC
a. REPORT U	b. ABSTRACT U	c. THIS PAGE U			19b. TELEPHONE NUMBER (include area code)

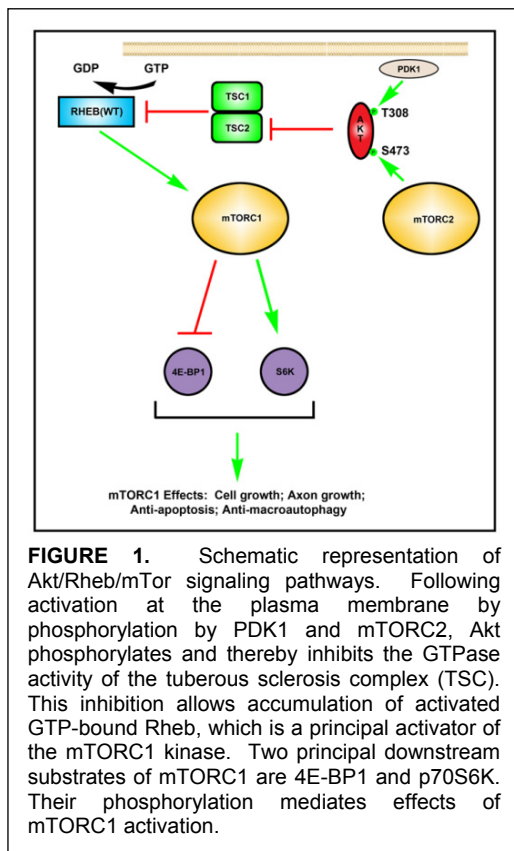
Table of Contents

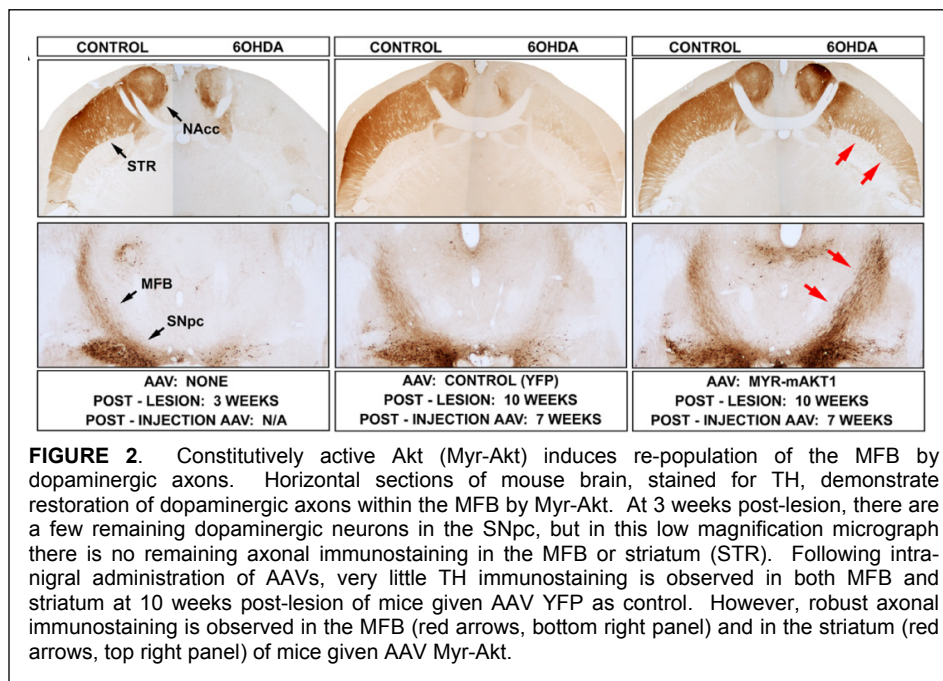
	<u>Page</u>
Introduction.....	2
Body.....	3
Key Research Accomplishments.....	8
Reportable Outcomes.....	9
Conclusion.....	9
References.....	9
Appendices.....	Padmanabahn et al, Gene Therapy, 2014, attached

INTRODUCTION

A longstanding concept in neuroscience has been that the mature mammalian central nervous system (CNS), unlike the peripheral nervous system (PNS), is incapable of axon regeneration. There are currently two principal concepts that form the basis of our understanding of the inability of the mature brain to regenerate axons. The first, and predominant, concept is that following injury to the CNS, extrinsic factors prevent axon growth (Benowitz and Yin, 2007; Raivich and Makwana, 2007). These extrinsic factors are principally of two types: glial scar and myelin breakdown products. The second concept to account for axon regeneration failure is that as the brain matures, the intrinsic developmental genetic programs that mediate axon growth are silenced. In recent years there has been growing interest in the role played by silencing in the adult brain of these intrinsic programs. The therapeutic promise offered by the concept of silencing of axon growth programs is that it suggests that if we are able to re-activate them, it may be possible to achieve long range restorative axon growth. Such a possibility has received support from our recent studies of the activation of Akt/mTor signaling in models of retrograde axonal degeneration induced by the dopaminergic neurotoxin 6-hydroxydopamine (6OHDA). In this model, 6OHDA is injected unilaterally into the striatum of mice and within one week it induces over 80% destruction of the dopaminergic nigro-striatal projection (Ries et al., 2008). This model has been used for many years to simulate the principal neurodegeneration that occurs in human Parkinson's disease (PD). In order to accurately simulate the clinical presentation of the disease, we waited until three weeks after the lesion, when most axons have been destroyed and about 50% of

neurons still survive, and then transduced the surviving dopamine neurons by use of an AAV1 vector with either a constitutively active mutant of the Akt kinase (myristoylated-Akt (MYR-Akt)) (Ries et al., 2006) or hRheb(S16H), a constitutively active mutant of the Rheb GTPase (Kim et al., 2011; Kim et al., 2012). Rheb GTPase is activated by Akt and it is a direct activator of the mTor kinase (Zoncu et al., 2011) (FIGURE 1). We have observed that transduction of SN dopamine neurons with either AAV MYR-Akt or AAV hRheb(S16H) induces a remarkable reinnervation of the striatum (FIGURE 2) (Kim et al., 2011; Kim et al., 2012). While these observations with AAV MYR-Akt and AAV hRheb(S16H) offer a promising proof-of-concept, they cannot be directly implemented as a gene therapy for humans because both of these molecules are potent oncogenes. The challenge, therefore, is to try to exploit the beneficial axon growth phenotype offered by this approach while eliminating the undesirable oncogenic phenotype. In this proposal, we seek to address this challenge by attempting to identify the critical mediators of the





axon growth phenotype downstream to mTor. We postulate that at some point downstream, the paths mediating the two phenotypes must diverge. Based on our results with hRheb(S16H) we know that activation of mTor is sufficient for axon growth. mTor has two principal substrates: eukaryotic translation initiation factor 4E binding protein (4E-

BP1) and p70S6K (FIGURE 1). Of the two, we hypothesize that p70S6K is more likely to play a role in axon growth. P70S6K has been identified as both necessary and sufficient for axon specification in primary neurons (Morita and Sobue, 2009). Transduction of neurons with a constitutively active form of p70S6K induced the formation of multiple axons, whereas increased expression of eIF-4E did not (Morita and Sobue, 2009). Although our principal hypothesis favors p70S6K in the induction of axon growth, we intend in this proposal to cover all possibilities by investigating the alternate mTor mediator, 4E-BP1, as well. The aim of this proposal therefore is to test the hypothesis that p70S6K or 4E-BP1 has the ability to induce axon regeneration in lesioned dopamine neurons. This proposal has direct therapeutic implication for the treatment of PD and other chronic neurologic diseases characterized by axon degeneration.

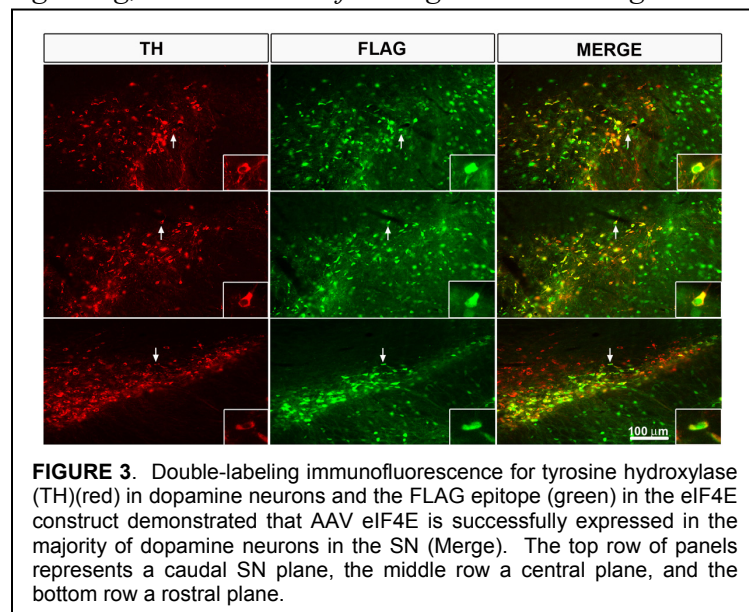
BODY

TASK 1 YEAR 01: To determine whether p70S6K or a constitutively active mutant, or both, are mediators of axon growth in the dopaminergic nigro-striatal projection.

In Year 01 we successfully completed this Task, and found that a constitutively active form of p70S6K can mediate new axon growth. In order to proceed, we first created the AAV vectors for p70S6K(WT) and the constitutively active form p70S6K(del C/T389E) (Yan et al., 2006; Sato et al., 2008). We next needed to determine whether these vectors were capable of successful transduction of dopamine neurons of the substantia nigra. This was done, and both vectors were found to have excellent transduction efficiency, without evidence of toxicity. After the viral vectors were created and characterized, we turned our attention to the performance of the Experiments outlined in TASK 1. In each of these Experiments a 6OHDA lesion was performed, followed in three weeks by intra-nigral injection of the AAV vectors. The effects on axon growth were assessed at 12 weeks post AAV, to allow enough time to fully assess the effects of the AAV injections. We determined by three measures that p70S6K(del C/T389E) induced new axon growth following their destruction by neurotoxin. We first determined that p70S6K(del C/T389E) partially restores axon numbers in the

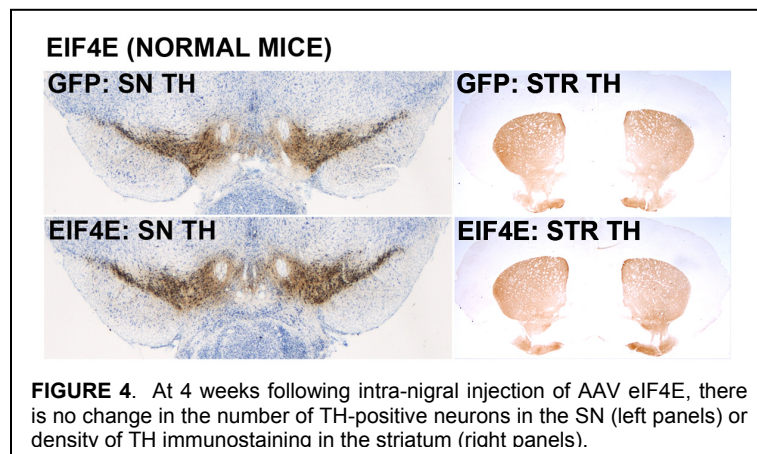
medial forebrain bundle (MFB), identified as TH-positive axons in the MFB. Examination of TH immunostaining alone is not an adequate assessment of new axon growth in this model, because restoration of the ability to express the TH protein may simulate the appearance of new axons when new growth has not in fact occurred. To address this concern, we used two methods. In the first, we used transgenic mice (TH-GFP) that express GFP under the TH promoter. Under the TH promoter, GFP is exclusively expressed in catecholaminergic neurons. GFP expression is more robust and more readily detected than endogenous TH, which must be demonstrated by immunostaining. Second we have used an anterograde tracer technique in which the axon-targeted fusion protein Tomato-Tau is delivered to SN neurons by AAV and expression is driven by the robust chicken-beta actin promoter, which is less likely to be subject to developmental regulation. These two methods can be performed simultaneously in the same mouse by injection of TH-GFP mice with AAV Tomato-Tau. By both methods there was a clear induction of axon growth by AAV p70S6K(del C/T389E). In order to determine whether these morphologic observations had a functional counterpart, we performed a behavioral analysis, using amphetamine-induced rotational behavior. Following unilateral 6OHDA lesion, the administration of amphetamine, which induces dopamine release, results in more release on the intact side and consequently rotations away from that side, towards the side of the lesion. In mice treated with AAV p70S6K(del C/T389E), this effect is reversed, indicating that nigro-striatal dopamine release has been restored on the lesioned side. Based on these results we concluded that our hypotheses was confirmed, that p70S6K, a downstream target of mTORC1, is capable of recapitulating the axon growth effects of MYR-Akt and hRheb(S16H).

TASK 2. YEAR 02. To determine whether 4E-BP1, as the second principal substrate of mTORC1 signaling, is a mediator of axon growth in the nigro-striatal dopaminergic projection.

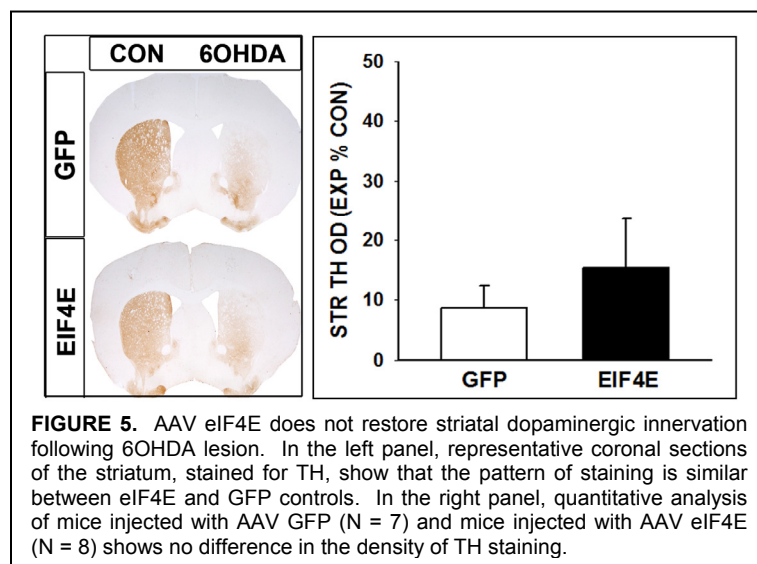


In Year 02 we first successfully created the AAV vector for eIF4E, a protein translation factor that is constitutively inhibited by 4E-BP1. In order to mimic the inhibitory effects of mTORC1 on 4E-BP1, the appropriate strategy is to overexpress eIF4E. As we did for the p70S6K constructs, we determined whether the vector was capable of successful transduction of dopamine neurons of the substantia nigra. The vector was found to have excellent transduction efficiency (FIGURE 3). We next assessed effects of the vector on

the dopaminergic nigro-striatal projection of normal, unlesioned mice, as a baseline, to make sure that there were no toxic effects, or, conversely, to see if they may have axon growth effects even in the absence of a lesion. This was done, and eIF4E was found to have no toxicity. It had no effect on dopaminergic neuron number in the SN, and, unlike p70S6K(del C/T389E), it had no effect on striatal dopaminergic innervation (FIGURE 4).



dopaminergic innervation of the striatum by tyrosine hydroxylase (TH) immunohistochemistry. The relative degree of innervation restored to the striatum was determined by measuring the optical density of staining on the lesioned side, and then



(TH) immunohistochemistry. The amount of axonal restoration was determined by stereologic counts of the number of axons on the lesioned side in comparison to the number of axons on the contralateral, intact, non-lesioned side. It can be seen in FIGURE 6 below that eIF4E did not induce a significant effect on the number of TH-positive axons in the MFB. In both of these studies AAV eIF4E differed from AAV p70S6K, studied in Year 1 of this proposal.

It is not sufficient to visualize axons by the expression of an endogenous protein such as TH. Such proteins may not be abundantly expressed either following injury or in the setting of new growth. Although it is important to visualize endogenous proteins, independent methods must also be used. We use two such methods. In the first, transgenic mice that express GFP under the TH promoter are used (TH-GFP mice). Axons are visualized and quantified by use of confocal microscopy to detect GFP fluorescence. In the second method, SN neurons are transduced with AAV Tomato-Tau, an anterograde anatomical marker of axons. Axons are visualized and quantified by use

With these studies completed, we proceeded with lesion experiments, as we proposed for TASK 2 in Year 02.

Briefly, for Experiment 1, mice received a unilateral intra-striatal 6OHDA lesion. At 3 weeks postlesion, they received either AAV eIF4E or AAV GFP by intra-nigral injection. At 12 weeks post AAV injection, mice were sacrificed for histological analysis of the striatum. It can be seen in FIGURE 5 that eIF4E did not induce a significant effect on striatal innervation. For Experiment 2, mice again received a unilateral intra-striatal 6OHDA lesion and at 3 weeks postlesion they received either AAV eIF4E or AAV GFP (as a control) by intra-nigral injection. At 12 weeks post AAV injection, mice were sacrificed for histological analysis of the number of dopaminergic axons within the medial forebrain bundle (MFB) by tyrosine hydroxylase

of confocal microscopy to detect Tomato fluorescence. In Experiment 3, TH-GFP transgenic mice received a unilateral intra-striatal 6OHDA lesion. At 3 weeks postlesion,

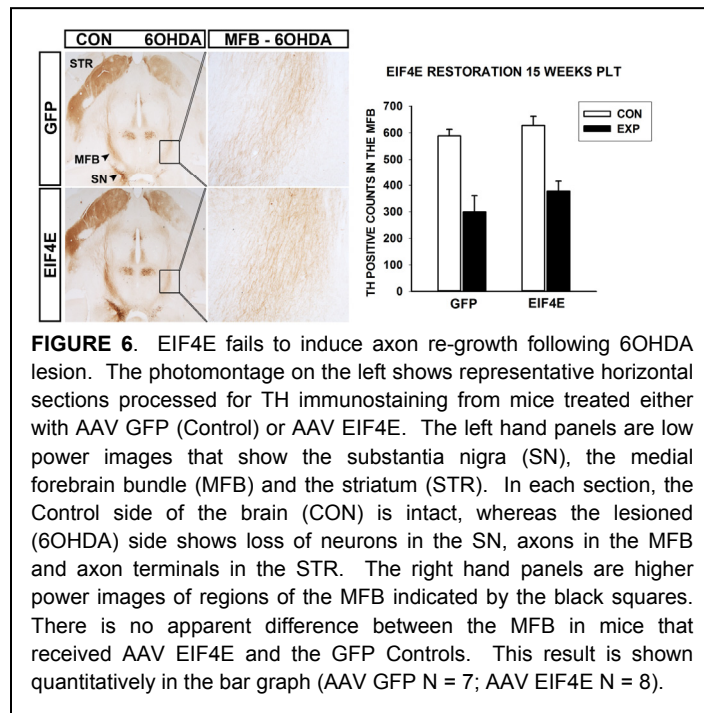


FIGURE 6. EIF4E fails to induce axon re-growth following 6OHDA lesion. The photomontage on the left shows representative horizontal sections processed for TH immunostaining from mice treated either with AAV GFP (Control) or AAV EIF4E. The left hand panels are low power images that show the substantia nigra (SN), the medial forebrain bundle (MFB) and the striatum (STR). In each section, the Control side of the brain (CON) is intact, whereas the lesioned (6OHDA) side shows loss of neurons in the SN, axons in the MFB and axon terminals in the STR. The right hand panels are higher power images of regions of the MFB indicated by the black squares. There is no apparent difference between the MFB in mice that received AAV EIF4E and the GFP Controls. This result is shown quantitatively in the bar graph (AAV GFP N = 7; AAV EIF4E N = 8).

they received either AAV eIF4E/AAV Tomato-Tau or AAV Tomato-Tau alone (as a control) by intra-nigral injection. At 12 weeks post AAV injection, mice were sacrificed for histological analysis of the number of dopaminergic axons within the medial forebrain bundle (MFB) by visualizing GFP. The amount of axonal restoration was determined by counts of the number of GFP-positive axons on the lesioned side in comparison to the number of axons on the contralateral, intact, non-lesioned side. It can be seen in FIGURE 7 below that eIF4E did not induce a significant effect on the number of GFP-positive axons in the MFB. In this Experiment axons were also visualized by use of the anterograde tracer, Tomato-Tau. It

can also be seen in FIGURE 7 that eIF4E did not induce a significant effect on the number of Tomato-Tau-positive axons in the MFB. In these results AAV eIF4E differs from AAV p70S6K, studied in Year 1 of this proposal.

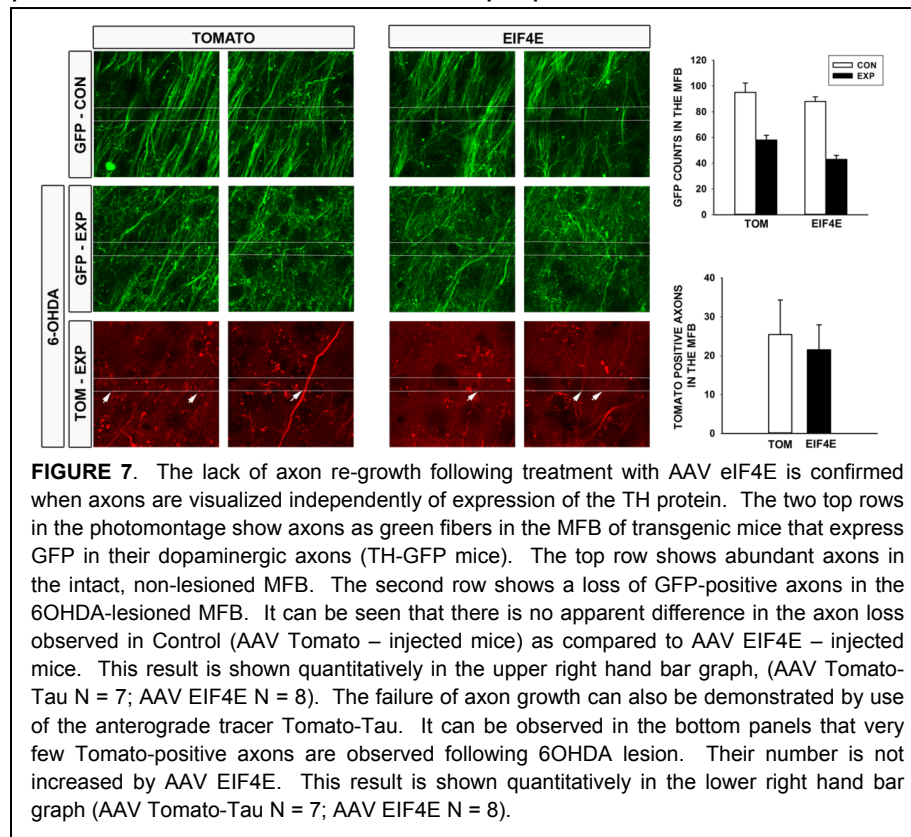
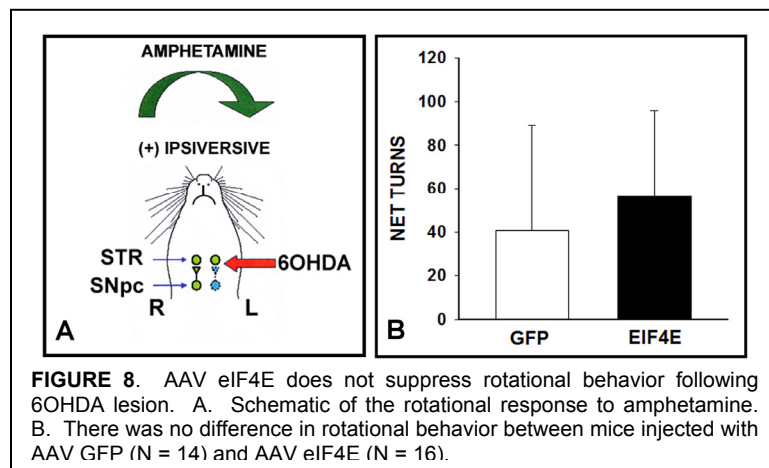
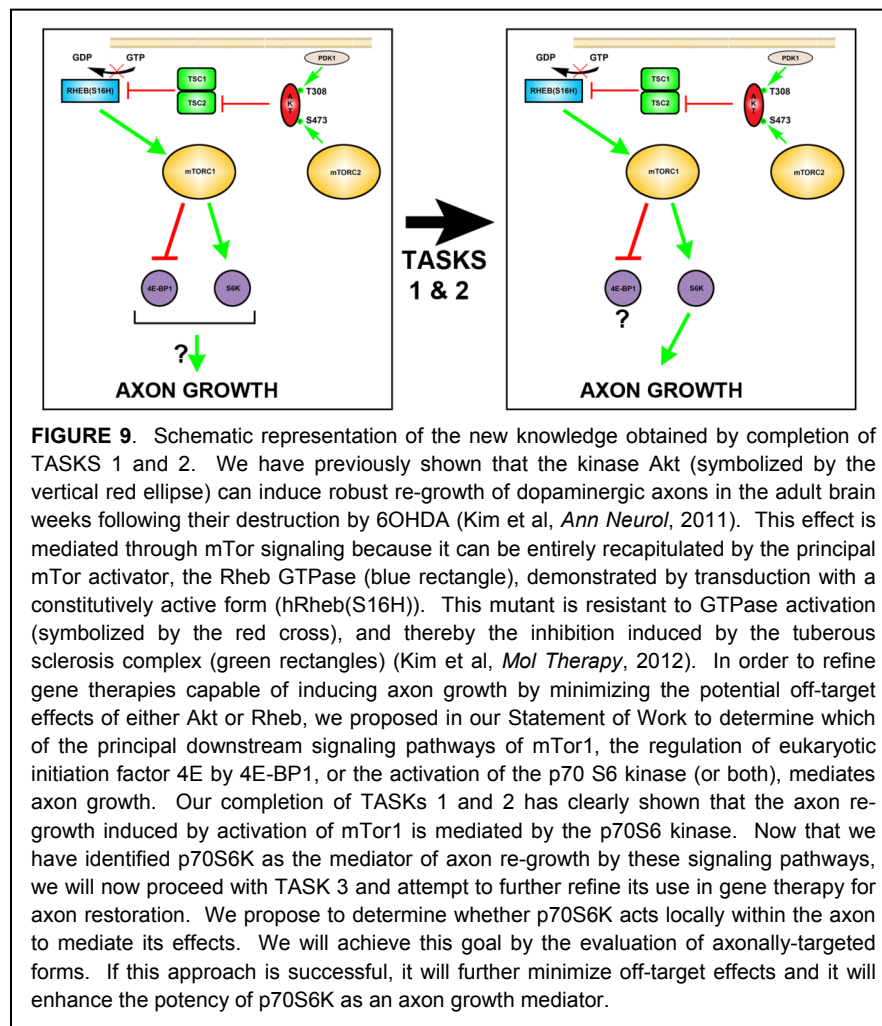


FIGURE 7. The lack of axon re-growth following treatment with AAV eIF4E is confirmed when axons are visualized independently of expression of the TH protein. The two top rows in the photomontage show axons as green fibers in the MFB of transgenic mice that express GFP in their dopaminergic axons (TH-GFP mice). The top row shows abundant axons in the intact, non-lesioned MFB. The second row shows a loss of GFP-positive axons in the 6OHDA-lesioned MFB. It can be seen that there is no apparent difference in the axon loss observed in Control (AAV Tomato – injected mice) as compared to AAV EIF4E – injected mice. This result is shown quantitatively in the upper right hand bar graph, (AAV Tomato-Tau N = 7; AAV EIF4E N = 8). The failure of axon growth can also be demonstrated by use of the anterograde tracer Tomato-Tau. It can be observed in the bottom panels that very few Tomato-positive axons are observed following 6OHDA lesion. Their number is not increased by AAV EIF4E. This result is shown quantitatively in the lower right hand bar graph (AAV Tomato-Tau N = 7; AAV EIF4E N = 8).

Given the lack of an effect of eIF4E on axon growth by these anatomical measures, we anticipated that there would not be evidence for restoration of behavioral deficits. It is important to point out that the behavioral assessment must be done, of course, while the animal is alive, prior to sacrifice for histological analysis. Thus, the behavioral data is obtained prior to knowledge of the anatomical results. For this Experiment, at 12 weeks post AAV injection, mice are



mice rotate ipsilaterally following administration of amphetamine as shown in FIGURE 8. If eIF4E partially restored dopaminergic innervation, it would be expected to also partially suppress this rotational behavior. However, it did not. This is not unexpected, given the lack of effect on striatal dopaminergic innervation. In this respect, it again differs from p70S6K which had a marked suppressive effect, as reported in Year 1.



administered amphetamine (2.5 mg/kg i.p.; Sigma) and placed in a plastic hemispherical bowl. Contralateral and ipsilateral turns are counted by a computerized rotometer system (San-Diego Instruments, San Diego, CA) for 60 min, and results are expressed as net turns per 60 min. In Control-treated mice, where there is an imbalance between the lesioned and non-lesioned striatum in the extent of dopaminergic innervation, the

With these results for AAV EIF4E completed in Year 02 we have come to an important juncture in our studies. We had originally proposed in our Statement of Work that we would devote our first two TASKs in Years 01 and 02 to a determination of which downstream substrate of the kinase mTor is responsible for its axon growth-mediating effects. After these first two years of work, and completion of TASKS 1 and 2 we have a clear and unequivocal answer: p70S6K mediates axon growth and eIF4E does not (FIGURE 9).

Now that we have made this determination, we will proceed in TASK3 to further refine the use of p70S6K by genetically

engineering it to be targeted to axons. We hypothesize that its axon growth effects are mediated locally within the axon. If our hypothesis is correct, then the axonally targeted forms will be more potent and it will have diminished risk of off-target effects, such as oncogenesis.

Now in Year 03, we have gone forward and created the following axon-targeting vectors for p70S6K(del C/T389E), the constitutively active form of p70S6K:

AAV cAPP-pS6K(CA): (CA: constitutively active). This construct is targeted to axons by 15 C-terminus amino acids of amyloid precursor protein (cAPP). cAPP was found in our recent publication in *Gene Therapy* (see below) to be the most effective known axon-targeting motif. In that study the motif was placed at the N-terminus as it had been in previously published studies.

AAV P70SK6(CA)-cAPP: This construct again uses the cAPP axon-targeting motif, but places it at the C-terminus as it is in its native location in the APP protein.

AAV cAPP-p70S6K(CA)-TAU-ZIP: This construct supplements the peptide-based cAPP axon targeting motif with an mRNA-based motif, the 3'UTR axon-targeting 'zip code' of the microtubule-binding protein tau. In our *Gene Therapy* publication, it was the most potent mRNA-based motif.

AAV 3XNLS-pS6K(CA): This construct includes a nuclear localization signal (NLS) and it will target the constitutively active form of p70S6K away from the axon, into the nucleus. It is a control construct.

AAV p70S6K(del C/T389E), the constitutively active form of p70S6K, without axonal targeting, will serve as a comparison control for the axonally targeted forms.

At present, in Year 03, we are making these constructs, and once they are produced, we will assess their ability to successfully transduce SN dopamine neurons. Once this is done, we will be able to directly compare their ability to induce new axon growth.

KEY RESEARCH ACCOMPLISHMENTS

- AAV2/1 vectors have been created for p70S6K(WT), p70S6K(del C/T389E), and eIF4E.
- All of these vectors have been shown to exhibit good transduction efficiency for dopaminergic neurons of the SN.
- AAV p70S6K(del C/T389E) has been shown to induce new axon growth in SN dopamine neurons following axon destruction, thus recapitulating the abilities of MYR-Akt and hRheb(S16H) to do so.
- The new axon growth induced by p70S6K(del C/T389E) is functional; it is able to restore behavioral deficits induced by 6OHDA lesion.
- AAV eIF4E does not recapitulate the axon growth effects of MYR-Akt and hRheb(S16H).

REPORTABLE OUTCOMES:

Padmanabhan S, Yarygina O, Kareva T, Kholodilov N, Burke RE. A constitutively active form of p70S6K induces axon growth in the nigrostriatal dopaminergic system. Society for Neuroscience, 2012.

Padmanabahn S, Kareva T, Kholodilov N, Burke RE. Quantitative morphological comparison of axon targeting strategies for gene therapies directed to the nigro-striatal projection. Gene Therapy, 2014, 21:115-122.

CONCLUSIONS

Based on our results in Years 01 & 02, we conclude that our fundamental strategy, to attempt to recapitulate the axon growth effects of MYR-AKT and hRheb(S16H) with mediators downstream of mTORC1 is successful, because we have achieved axon growth with a constitutively active form of p70S6K. In Year 02 we determined that the other principal mTor target, eIF4E, does not have axon growth induction capacity. In completing our studies of p70S6K, we noted that although p70S6K(del C/T389E) has clear axon growth effects, they do not seem to be as robust as hRheb(S16H), our most potent lead molecule to date. We therefore in Year 03, will develop the axon-targeting strategy proposed for TASK 3. We anticipate that axon targeting will enhance the efficacy of our lead second generation molecules without adding to their oncogenic potential.

REFERENCES

- Benowitz LI, Yin Y (2007) Combinatorial treatments for promoting axon regeneration in the CNS: strategies for overcoming inhibitory signals and activating neurons' intrinsic growth state. *Dev Neurobiol* 67:1148-1165.
- Kim SR, Kareva T, Yarygina O, Kholodilov N, Burke RE (2012) AAV Transduction of Dopamine Neurons With Constitutively Active Rheb Protects From Neurodegeneration and Mediates Axon Regrowth. *Mol Ther* 20:275-286.
- Kim SR, Chen X, Oo TF, Kareva T, Yarygina O, Wang C, During MJ, Kholodilov N, Burke RE (2011) Dopaminergic pathway reconstruction by Akt/Rheb-induced axon regeneration *Ann Neurol* 70 110-120.
- Morita T, Sobue K (2009) Specification of neuronal polarity regulated by local translation of CRMP2 and Tau via the mTOR-p70S6K pathway. *J Biol Chem* 284:27734-27745.
- Raivich G, Makwana M (2007) The making of successful axonal regeneration: genes, molecules and signal transduction pathways. *Brain Research Reviews* 53:287-311.
- Ries V, Henchcliffe C, Kareva T, Rzhetskaya M, Bland RJ, During MJ, Kholodilov N, Burke RE (2006) Oncoprotein Akt/PKB: Trophic effects in murine models of Parkinson's Disease. *Proc Natl Acad Sci USA* 103:18757-18762.
- Ries V, Silva RM, Oo TF, Cheng HC, Rzhetskaya M, Kholodilov N, Flavell RA, Kuan CY, Rakic P, Burke RE (2008) JNK2 and JNK3 combined are essential for apoptosis in dopamine neurons of the substantia nigra, but are not required for axon degeneration. *J Neurochem* 107:1578-1588.

- Sato T, Umetsu A, Tamanoi F (2008) Characterization of the Rheb-mTOR Signaling Pathway in Mammalian Cells: Constitutive Active Mutants of Rheb and mTOR. *Methods Enzymol* 438:307-320.
- Yan L, Findlay GM, Jones R, Procter J, Cao Y, Lamb RF (2006) Hyperactivation of mammalian target of rapamycin (mTOR) signaling by a gain-of-function mutant of the Rheb GTPase. *J Biol Chem* 281:19793-19797.
- Zoncu R, Efeyan A, Sabatini DM (2011) mTOR: from growth signal integration to cancer, diabetes and ageing. *Nat Rev Mol Cell Biol* 12:21-35.

ENABLING TECHNOLOGIES

Quantitative morphological comparison of axon-targeting strategies for gene therapies directed to the nigro-striatal projection

S Padmanabhan¹, T Kareva¹, N Kholodilov¹ and RE Burke^{1,2}

Cellular targeting of mRNAs and proteins to axons is essential for axon growth during development and is likely to be important for adult maintenance as well. Given the importance and potency of these axon-targeting motifs to the biology of axons, it seems possible that they can be used in the design of transgenes that are intended to enhance axon growth or maintenance, so as to improve potency and minimize off-target effects. To investigate this possibility, it is first essential to assess known motifs for their efficacy. We have therefore evaluated four axon-targeting motifs, using adeno-associated viral vector-mediated gene delivery in the nigro-striatal dopaminergic system, a projection that is predominantly affected in Parkinson's disease. We have tested two mRNA axonal zipcodes, the 3' untranslated region (UTR) of β -actin and 3' UTR of tau, and two axonal-targeting protein motifs, the palmitoylation signal sequence in GAP-43 and the last 15 amino acids in the amyloid precursor protein, to direct the expression of the fluorescent protein Tomato in axons. These sequences, fused to Tomato, were able to target its expression to dopaminergic axons. Based on quantification of Tomato-positive axons, and the density of striatal innervation, we conclude that the C-terminal of the amyloid precursor protein is the most effective axon-targeting motif.

Gene Therapy advance online publication, 5 December 2013; doi:10.1038/gt.2013.74

Keywords: Parkinson's disease; APP; axon; targeting; gene therapy; AAV

INTRODUCTION

The complex circuitry of the central nervous system is made possible by the unique, highly polarized cellular anatomy of individual neurons. In the case of axons, the cellular polarization can be extreme. Even in relatively compact projections, the arborization of axon terminal fields can create an axonal volume that dwarfs that of the cell body, as, for example, in the case of nigro-striatal projection neurons.¹ This unique anatomy of axons creates unique cellular demands. There is growing evidence that neurons meet these demands by targeting some proteins and mRNAs to the axon, the latter to undergo local intra-axonal translation.²

Cellular targeting to axons has gained recognition as important to a variety of axonal functions, such as pathfinding,³ and it may have a role in the pathogenesis of some degenerative neurological disorders.⁴ Given the evidence that some axonal functions, such as elongation, may be mediated at the intra-axonal level, axon-targeting motifs may also find use in gene therapies intended to restore axonal projections by induction of re-growth.^{5,6}

Axon-targeting motifs have been identified in both mRNA ('zipcodes') and peptide sequences. Zipcodes (or cis-acting elements) are sequences in the 5' or 3' untranslated region (UTR) of the mRNA that interact with mRNA-binding proteins (or trans-acting factors) and mediate mRNA transport to the translational site within the axon. One of the first identified mRNA zipcodes is a 54nt sequence in the 3' UTR of β -actin mRNA.^{2,7} This sequence was determined to be essential for the localization of β -actin to the leading lamellae of fibroblasts, and it was subsequently shown to be necessary for β -actin localization to growth cones.⁸ Microtubule-associated protein, tau, is a

neuron-specific protein that is found primarily in axons. A 241nt AU-rich region in the 3' UTR of tau mRNA is required for axonal expression of both tau mRNA and protein in differentiated P19 cells⁹ indicating that it serves as an axonal zipcode. Based on the above literature, we evaluated two mRNA zipcodes (the zipcodes in β -actin and tau) for their ability to target axons.

We also evaluated two axon-targeting peptide sequences: the N-terminal palmitoylation signal of growth-associated protein (GAP-43) and the C-terminal 15 amino acids of the amyloid precursor protein (APP, a membrane-associated protein). Fusion of the palmitoylation motif of GAP-43 to green fluorescent protein (GFP) is sufficient to target it preferentially to axons.¹⁰ Moreover, when single-dopamine neurons of the substantia nigra (SN) were transduced with GFP bearing the palmitoylation sequence of GAP-43, extensive axonal arborization in the striatum of the single transfected neuron was observed.¹ The axonal-targeting motif of the last 15 amino acids in the C terminus of APP was first identified by observing its association with transported herpes simplex virus particles.¹¹

In this study, we tested the efficacy of these axon-targeting motifs to target the fluorophore tdTomato to the axons of the nigro-striatal pathway, a pathway that is predominantly affected in Parkinson's disease, following transduction with adeno-associated viral vectors.

RESULTS

Generation of the plasmids for the control and axon targeted viral vectors

The different mRNA and protein sequences were amplified as discussed in the Materials and Methods section. All constructs

¹Department of Neurology, Columbia University Medical Center, New York, NY, USA and ²Department of Pathology and Cell Biology, Columbia University, New York, NY, USA. Correspondence: Dr RE Burke, Department of Neurology, Columbia University Medical Center, 650 West 168th Street, Room 306, New York, NY 10032, USA.

E-mail: rb43@columbia.edu

Received 26 July 2013; revised 10 October 2013; accepted 29 October 2013

were subcloned into an adeno-associated virus 2 (AAV2) backbone plasmid (pBL) that incorporated the chicken β -actin promoter and a woodchuck post-transcriptional regulatory element.⁶ The different targeting motifs were inserted either at the 5' or 3' end of the coding sequence for tdTomato to generate Tomato-CaMKII-zip, Tomato- β -actin-zip, Tomato-Tau-zip, GAPpal (palmitoylation signal of GAP-43)-Tomato and cAPP (C-terminal of APP)-Tomato (see schematic in Figure 1).

Expression of axon-targeting viral vectors in the substantia nigra pars compacta (SNpc) dopamine neurons

All vectors were first evaluated for any evidence of toxicity to dopamine neurons of the SNpc in adult C57BL/6 mice. At 4 weeks post injection, these neurons were visualized by tyrosine hydroxylase (TH) immunoperoxidase staining with a thionin counterstain (Supplementary Figure 1). The uninjected side served as an internal control. Neither loss of dopamine neurons in the SN nor the presence of an inflammatory cellular infiltrate was observed with any of the vectors. In a pilot study, we compared the efficiency of the two axon-targeting 3' UTR mRNA zipcodes, the β -actin-3' UTR^{2,7,8} and tau-3' UTR,⁹ to target Tomato fluorescence to dopaminergic terminal fields. In comparison to Tomato-tau-zip, Tomato- β -actin-zip showed minimal Tomato fluorescence in the striatum indicating less targeting. Therefore, the β -actin-3' UTR zipcode was not further evaluated (Supplementary Figure 2).

In this study, we transduced dopamine neurons in the SNpc with the different viral vectors and monitored the expression of Tomato at different levels of the nigrostriatal projection system. The principal axonal tract of the dopamine neurons in the SNpc lies within the medial forebrain bundle (MFB) and these axons terminate in the striatum (Figure 2a). Transduction of the SNpc by each vector was assessed by both fluorescence and immunoperoxidase staining of Tomato in coronal mesencephalic sections (Figure 2b). The fibers observed around the cell bodies in the SNpc and the fibers descending into the substantia nigra pars reticulata are predominantly dendrites. Both control and axon-targeting vectors labeled cell bodies (indicated by asterisk in the inset panels) and fibers in the SN (see Figure 2b the inset panels). However, the dendrites in the substantia nigra pars reticulata are extensively labeled with the Tomato-CaMKII-zip construct thus validating that the zipcode in CaMKII causes preferential targeting of Tomato to dendrites. In order to quantitatively compare numbers of cells transduced in the SN by the different vectors, we performed stereology on complete sets of serial sections immunoperoxidase stained for Tomato. Although the fluorescence images gave us striking images of the different regions of the nigrostriatal circuitry where the viral vectors were targeted, we relied on immunoperoxidase staining to quantify the results. We found that the number of neurons in the SNpc transduced by the different vectors was comparable with the exception of Tomato-CaMKII-zip (Figure 2c), which showed significantly fewer SNpc Tomato-positive counts.

At the population level within the SN, the pattern of transduction by these vectors corresponded to the distribution of the SNpc, which is predominantly dopaminergic. To confirm expression by these vectors in dopaminergic neurons, we examined cellular expression of Tomato in transgenic mice with GFP expression under the control of the rat TH promoter. This analysis confirmed extensive co-expression of Tomato and GFP in neurons of the SNpc; single examples for each vector are shown in Figure 3.

Relative efficacy of axon targeting viral vectors

In order to compare the ability of these vectors to target the expression of Tomato to the axons of dopaminergic neurons, we performed two assessments: (1) the number of Tomato-positive

Tomato



Tomato-CaMKII-zip



ratCaMKII α -zip

```
GATCCCTGTCTGCACTGTTTCTTTGCATGACTTTATATGCAGTAAGTA
TGTTGAGAAAAAAGAGACAAAGACAAAAAAGAAAAACACTCAG
CAAAATCAAACGACACGTTTGGACAAAAATATAATAAACATTCA
AGTTATATTCTCAGTGTCACCTTGAATTACGTTGCTGCCTCTCTGT
GCTTTTGGTCTCTGTGTGGCTGTGTTTGGCAGCATGAGACCCTGTCCC
CTCTGGAGGTTTCTAGGGGAGGAAGACCGTGTGTCGGGGGGGGGT
TGGAGACAGCTTTGCTCTCAGCTTTTGGGGGGGGTGGATTGGAGC
AGAAGTGGAGGGGATGTTAATCCAGAACTTTCTGGTATTTCCTTTC
TCCACGCAGTGAGCTATACGCTGGGCTCTCTCTCAAACTCTGCTGC
CCAGGGACAAGTATAGGGTGAAGGGTGGCCCTATTGTCTAAGCCAC
TCCACTGTAGCCCTCTGCCTTTGGTAGAGACACTGTACCCAGACCCA
AGATGGGCCCTTGTCCACCC CAGATC
```

Tomato- β -actin-zip



Chicken β -actin-zip

```
ACCGGACTGTTACCAACACCCACCCCTGTGATGAAACAAACCCATA
AATGC
```

Tomato-Tau-zip



ratTau-zip

```
GGCGCCATCGTGGATGGGAGTCCGTGTGTGCTGGAGATTACCTGG
ACACCTCTGCTTTTTTTTTTTTACTTTAGCGGTTGCCTCTAGGCCTGAC
TCCTTCCCATGTTGAAGTGGAGGACGACGTTAGGTGTCAATGTCTC
GGCATCAGTATGAACAGTCAGTAGTCCAGGGCAGGGCCACACTTCT
CCCATCTTCTGCTTCCACCCAGCTGTGATTGTAGCTCCAGAGCT
```

GAPpal-Tomato



mouseGAPpal

```
ATGCTGTGCTGTATGAGAAGAACCAACAGGTTGAAAGAAATGATGAG
GACCAAAAGATT
```

cAPP-Tomato



mousecAPP

```
GGATATGAGAATCCAACCTACAAGTTCTTTGAGCAAATGCAGAAC
```

Figure 1. Schematic representation of axon-targeting viral vector constructs and controls. Each construct is shown within the AAV-2-based pBL vector backbone, in which colored boxes represent the following elements of the plasmid: ITR, inverted terminal repeat (green), CBA, chicken β -actin promoter (yellow); WPRE, woodchuck hepatitis virus posttranscriptional regulatory element (blue). The axon-targeting sequences (represented by the solid gray boxes) were incorporated into a construct containing the coding sequence of the fluorophore tdTomato as indicated. cAPP, C-terminal of the amyloid precursor protein; GAPpal, GAP-43 palmitoylation signal; Zip, zipcode.

axons in the MFB, the principal projection system of dopamine neurons of the SNpc; and (2) the abundance of Tomato expression in the striatum.

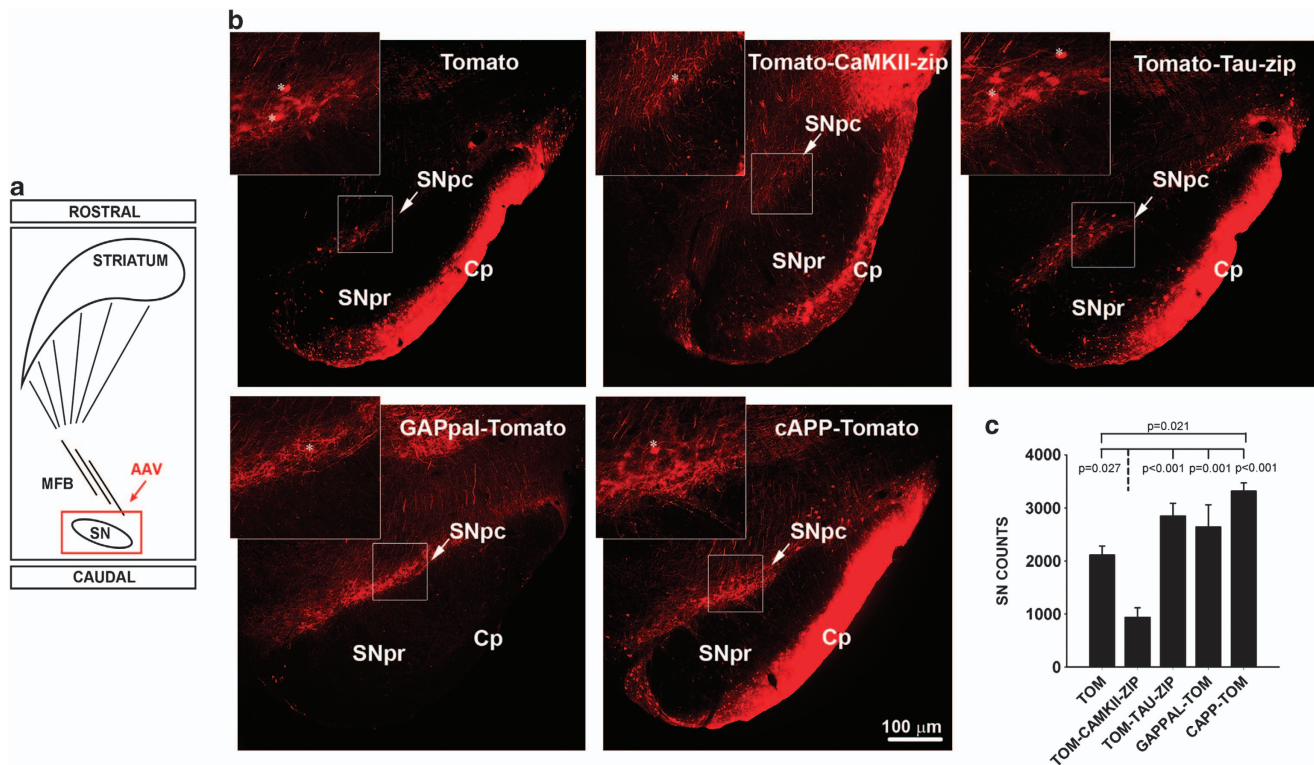


Figure 2. Transduction of the substantia nigra pars compacta (SNpc) by axon-targeting viral vectors and controls. (a) Schematic of the nigrostriatal circuitry demonstrates the location of the cell bodies of the dopaminergic neurons in the SN where the AAVs were injected. (b) Tomato fluorescence demonstrates the expression of each axon-targeting vector in the SNpc 4 weeks post viral injection. Scale bar = 100 μm. Each inset shows the SNpc at a higher magnification of the boxed area. The asterisks in the inset panels are example of cell bodies that are Tomato positive in the SNpc. (c) For quantitative analysis, coronal sections of the SNpc were immunoperoxidase stained for Tomato and the number of positive neurons was determined by stereological analysis. The bars in the graph show mean values for neuron number ($n = 5$ animals for each viral vector; error bars represent s.e.m.). The Tomato-CaMKII-zip vector showed significantly fewer transduced neurons ($P < 0.001$ analysis of variance, P values as indicated by Tukey *post hoc*). The numbers of vector genomes injected per mouse were 2×10^9 for AAV-Tomato, 1×10^9 for AAV-Tomato-CaMKII-zip, 4×10^9 for AAV-Tomato-Tau-zip, 6×10^9 for AAV-GAPpal-Tomato and 4×10^9 for AAV-cAPP-Tomato. AAV, adeno-associated virus; Cp, cerebral peduncle; MFB, medial forebrain bundle; SNpr, substantia nigra pars reticulata.

The different control and axon-targeting viral vectors were injected into the SNpc of TH-GFP mice and 4 weeks later, the axons in the MFB were quantified. TH-GFP mice are suitable for this analysis as the entire population of dopaminergic axons in the MFB is labeled. Using the GFP-positive axons to delineate the MFB, we were able to quantify the number of Tomato-positive axons in the MFB for each construct. The MFB consists predominantly of axons, and hence, any fiber that is labeled in the MFB can be considered to be an axon. Expression of the different control and axon-targeting viral vectors in two fields of the MFB is represented (Figure 4b). Tomato lacks any targeting sequence, and hence, the fluorescence observed in the MFB is considered as the baseline targeting of the viral vectors to axons. On the other hand, Tomato-CaMKII-zip is expected to target Tomato to the dendrites, and hence, very few axons in the MFB should be observed. Assessment of Tomato-positive axon numbers in the MFB revealed that control vectors Tomato and Tomato-CaMKII-zip labeled few axons as anticipated. All three axon-targeting viral vectors showed higher axonal counts when compared with the control vectors (Figure 4b panels to the right). Among them, cAPP-Tomato demonstrated the greatest number of Tomato-positive axons in the MFB, about threefold the number observed in controls (Figure 4c). In order to determine whether cAPP-Tomato was indeed superior to the other axon-targeting constructs in its ability to target Tomato to the axons, we also evaluated the axon numbers (Tomato-positive counts in the MFB) after normalization by the total number of axons in the MFB (GFP-positive counts in the MFB).

Although Tomato-CaMKII-zip labeled very few dopaminergic axons in the MFB, cAPP-Tomato revealed striking co-expression of Tomato and GFP in the MFB (Figure 5a). Normalization of the Tomato-positive axons to the total number of dopaminergic axons (GFP-positive) in the MFB shows that all three axon-targeting viral vectors label higher number of dopaminergic axons in the MFB as compared with the control vectors (Figure 5b). However, the effect observed with cAPP-Tomato was significant and threefold higher as compared with the controls. Consideration was given to the possibility that dendrites arising from neurons adjacent to the MFB may be incorrectly identified as axons by tomato labeling. However, this is unlikely for two reasons. The AAV injections were made directly into the SN and tomato labeling of neurons in the MFB does not occur. Second, dendritic morphology is distinguishable from axonal morphology; dendrites generally taper and branch as they extend away from the soma, whereas dopaminergic axons in the MFB do not.¹

Expression of Tomato in the striatum was assessed in coronal sections by both epifluorescence and by determination of the density of immunoperoxidase staining. The Tomato and Tomato-CaMKII-zip constructs labeled very few fibers in the striatum by Tomato fluorescence, whereas the axon-targeting vectors showed abundant Tomato-positive fibers (Figure 6a). At a higher power, individual fibers and dense terminal arborizations were observed in the case of GAPpal-Tomato and cAPP-Tomato. In order to confirm these observations, we performed Tomato immunoperoxidase staining. Striatal Tomato optical density was higher for

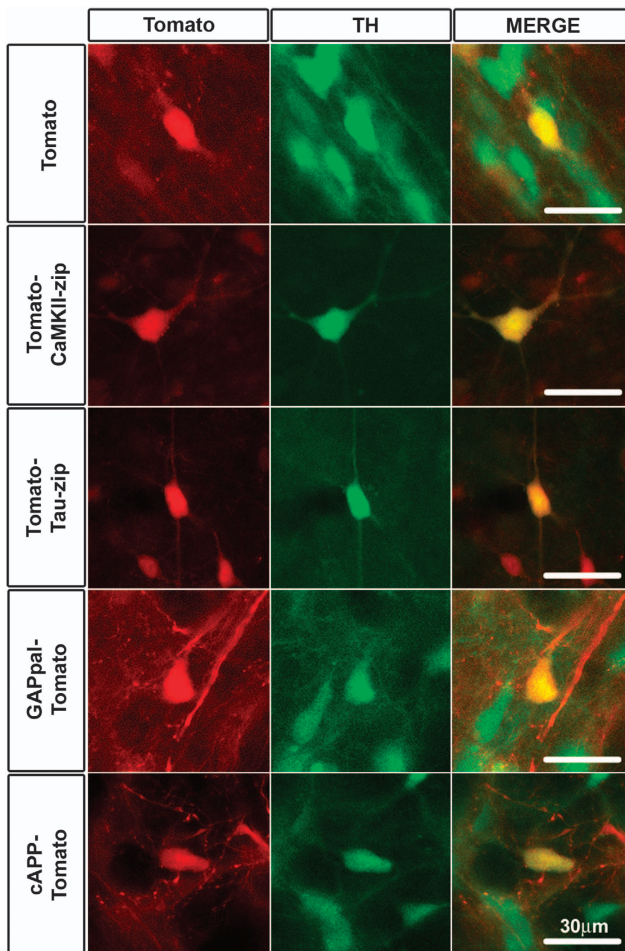


Figure 3. Transduction of dopamine neurons in the SNpc by the axon-targeting viral vectors and controls. Mice expressing GFP under the TH promoter were injected with the Tomato-tagged axon-targeting viral vectors and 4 weeks later horizontal sections were obtained. Representative epifluorescence images confirm expression of each transgene within dopamine neurons of the SNpc. Scale bar = 30 μ m. TH, tyrosine hydroxylase.

the three axon-targeting vectors compared with the control vectors. Of the three axon targeting viral vectors, cAPP-Tomato showed the highest optical density measurements, in keeping with the results obtained for Tomato-positive axon counts in the MFB (Figure 6b).

Both the number of axons in the MFB and striatal immunoperoxidase-labeling density are directly related to transduction efficiency. We therefore normalized the measurements obtained for striatal optical density to the number of neurons that were transduced in the SNpc for each viral vector. This ratio would take into account differences in viral titer and differences in the transduction efficiency of each viral vector. This ratio was higher for Tomato-Tau-zip, GAPpal-Tomato and cAPP-Tomato than the controls and, in the case of cAPP-Tomato, it was significantly higher than any other viral vector (Figure 6c). Thus, by all assessments, cAPP was identified as the most effective axon-targeting sequence. Excessive accumulation of Tomato (especially with the axonally targeted constructs) in the striatum could lead to subtle toxicity over the 4-week period. In order to rule out this possibility, we performed TH immunostaining in the striatum after the different viral vector injections and measured the TH optical density in the striatum. Our results indicate no toxicity as the values for TH striatal optical density were similar with the

different control and axon-targeting viral vectors (Supplementary Figure 3).

DISCUSSION

This study shows that the C-terminus axon-targeting sequence of the amyloid precursor protein is sufficient and most effective to target the fluorophore tdTomato to the axons in the nigro-striatal dopaminergic system. Our assessment is based on two distinct but complementary measurements of Tomato expression in the axons and terminal fields of the nigro-striatal projection. The most direct method, the counting of Tomato-positive axons in the MFB, has the advantage of direct axon visualization, but the limitation that once the threshold of expression required for visualization of the individual axon is achieved, further increases in expression in that axon are not measured. Our second method of assessment, the determination of the optical density of immunoperoxidase staining for Tomato in the striatum, does not visualize axons in terminal branches at the individual fiber level, but remains responsive to increases in Tomato protein beyond the threshold of visualization of fibers. By both of these methods of assessment, these axon-targeting motifs induced augmented expression of Tomato transgene in nigro-striatal axons and terminal fields.

The superior efficacy of cAPP by both the MFB axon counts and striatal optical density measures was not due simply to greater efficiency in the transduction of neurons of the SNpc, because there was no difference between cAPP and the GAPpal sequence or the tau mRNA zipcode in this respect. Furthermore, when striatal immunoperoxidase optical density values were normalized for the number of transduced SN neurons, cAPP still showed a superior ability to target axons. Our observations confirm those of Babetto and colleagues¹² made *in vivo* that cAPP is an effective axon-targeting motif.

In our study, the axon-targeting motifs were fused to Tomato either at the N or at the C terminus based on previous studies that first validated these sequences. Whether N- or C-terminus localization of these sequences will have different effects on targeting remains to be studied. A recent study by Biemann *et al.*¹³ showed that a pair of Sushi domains in the N-terminal of the GABA_{B1a} is sufficient to target the somatodendritic mGluR1a protein to axons. Whether these domains may also target proteins of interest into axons in the nigrostriatal dopaminergic system remains to be evaluated.

Although the cAPP amino-acid sequence was the most effective axon-targeting motif in our analysis, our data are not intended to suggest a broader conclusion that, in general, peptide motifs are more effective than mRNA zipcode motifs, such as those found in the β -actin and tau mRNAs. Our observations indicate that both mRNA and protein axonal-targeting motifs can be used to augment the expression of transgenic proteins in axons in brain *in vivo*. The tau 3' UTR zipcode motif showed strong trends for increased axonal localization of Tomato in comparison to control in MFB axon counts, striatal optical density and optical density normalized for SN neuron counts. We therefore anticipate that with more extensive study, the tau 3' UTR zipcode will prove to be an effective axon-targeting motif. Axonal targeting at the mRNA level has the distinct advantage that the protein will be synthesized locally in the axon, and therefore more likely to have a selective axonal localization. Proteins with axon-targeting motifs, synthesized in the cell body, may contain competing targeting motifs, or post-translational modifications, that may target them to other cellular structures or compartments. Protein-targeting sequences, on the other hand, could be advantageous as they do not rely on the expression and availability of mRNA-binding proteins that are essential for the precise targeting of the mRNA zipcodes to the axons.^{14–16} With either mRNA or peptide motifs, we failed to exclude Tomato from the cell body suggesting that achieving expression solely within the axons is improbable.

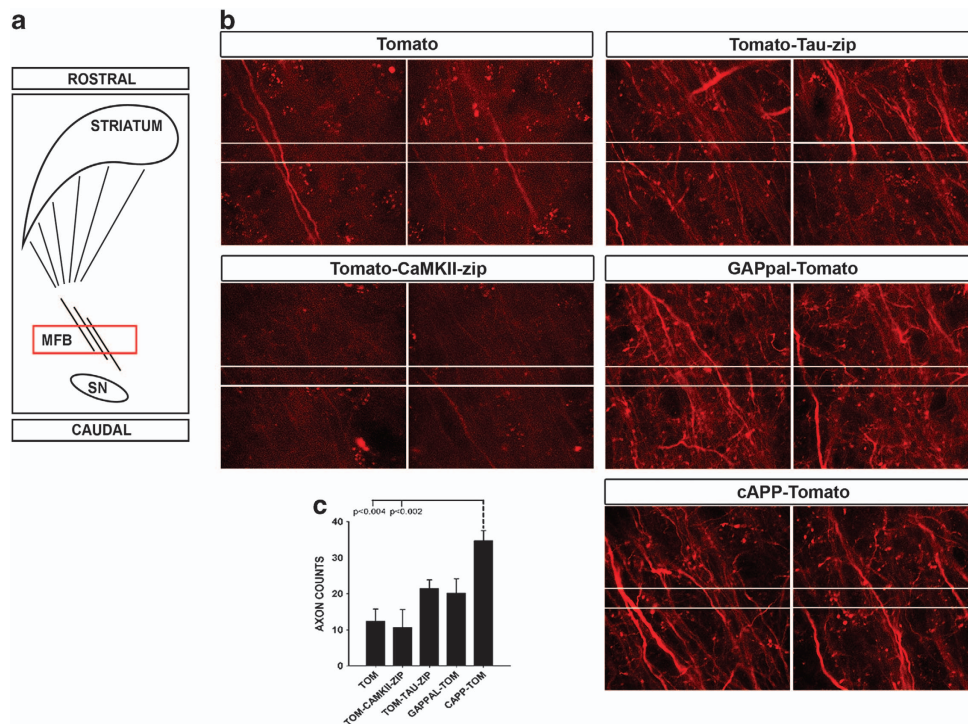


Figure 4. Expression of Tomato by axon-targeting vectors and controls in axons of the medial forebrain bundle (MFB). **(a)** Schematic of the nigrostriatal circuitry indicates the axons of the SN dopaminergic neurons in the MFB. **(b)** Representative confocal images of Tomato fluorescence in two lateral fields of the MFB are demonstrated for each viral vector. GFP fluorescence (not shown) was used to localize the MFB in each section. Each panel represents a z-axis maximal projection of 20 confocal optical planes through a 2- μ m vertical distance within the MFB. **(c)** Quantitative analysis of the number of Tomato-positive axons for each construct. Significantly more axons were demonstrated by cAPP-Tomato in comparison to controls ($P=0.002$ analysis of variance, P values as indicated by Tukey *post hoc*; $n=4$ animals for each viral vector). The numbers of vector genomes injected per mouse were the same as that specified in Figure 2.

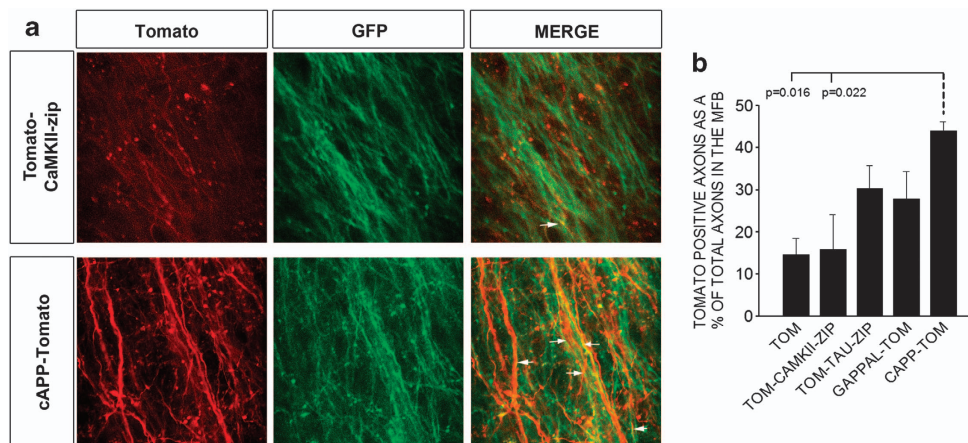


Figure 5. Relative expression of Tomato in the axons of the MFB. **(a)** Representative confocal images of Tomato and GFP fluorescence in one of the fields of the MFB are demonstrated for one control (Tomato-CaMKII-*zip*) and one axon-targeting (cAPP-Tomato) vector. The Tomato panels indicate the number of axons in the MFB that are labeled by the control and axon-targeting viral vectors, whereas the GFP panels demonstrate the total number of dopaminergic axons in the field. The panels are z-stack maximal projection images of 20 confocal optical planes through a 2- μ m vertical distance within the MFB. **(b)** Quantitative analysis of the number of Tomato and GFP-positive axons for each construct. Every axon transecting the two lines set 10 μ m apart in the caudal to rostral dimension (shown as two horizontal white lines in **a**) were counted. When the Tomato-positive axons were expressed as a percentage of GFP-positive axons, cAPP-Tomato showed the greatest amount of co-expression ($P=0.013$ analysis of variance, P values as indicated by Tukey *post hoc*; $n=4$ animals for each viral vector).

However, with this approach, the ratio of Tomato fluorescence observed in the axon to that observed in the cell body is greatly enhanced with the axon-targeting motifs as evidenced by the Tomato-positive axon counts in the MFB and the SNpc.

Our goals in performing the assessment of axon-targeting motifs were not only to establish their ability to target axons but

also to provide methodological approaches to quantifying and comparing their relative efficacy. The two measures that we have used, MFB axon counts and striatal optical density, are complementary and yet confirmatory, because they identified the same rank order of potency: cAPP > GAPpal > tau *zip* > Tomato controls. This analysis therefore provides a proof-of-principle for the

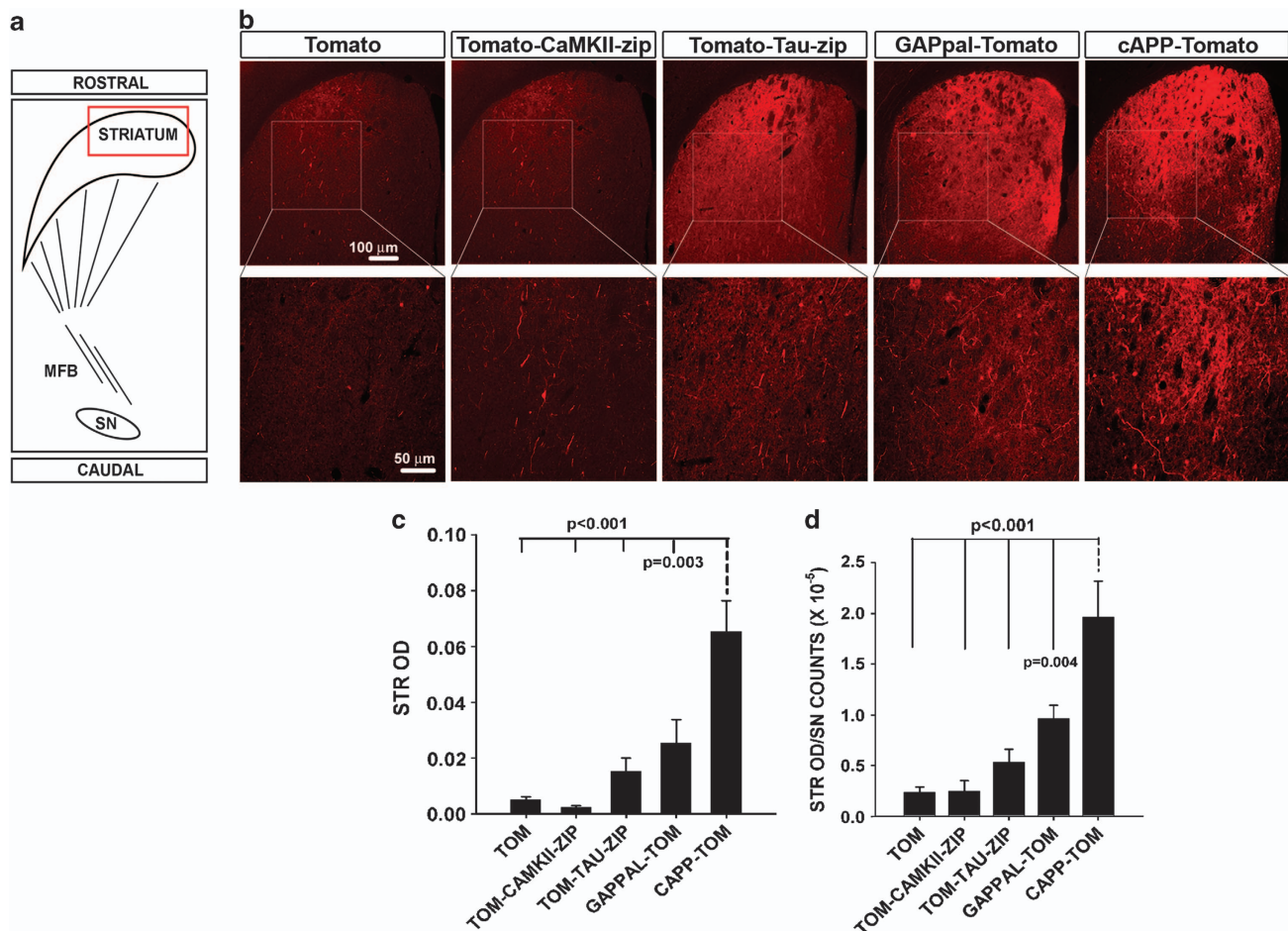


Figure 6. Expression of Tomato by axon-targeting viral vectors and controls in the striatum. **(a)** Schematic of the nigro-striatal circuitry demonstrates the dopaminergic axon terminals in the striatum where the observations were made. **(b)** Epifluorescence images demonstrating expression of Tomato in the striatum for each vector. Scale bar = 100 μ m. The lower panels show magnified images of the area boxed in the upper panels. Scale bar = 50 μ m. **(c)** Quantitative analysis of the optical density of Tomato immunoperoxidase staining in the striatum, 4 weeks post viral injection. cAPP-Tomato demonstrated significantly more striatal expression than all other constructs ($P < 0.001$ analysis of variance (ANOVA), P values as indicated by Tukey *post hoc*; $n = 5$ for each viral vector). **(d)** The ratio of Tomato optical density in the striatum to Tomato-positive neurons in the SNpc for each viral vector is shown. When normalized for the number of positive neurons in the SNpc, the striatal optical density for cAPP-Tomato remains significantly greater than all other constructs ($P < 0.001$ ANOVA, P values as indicated by Tukey *post hoc*; $n = 5$ animals for each viral vector). The numbers of vector genomes injected per mouse were the same as that specified in Figure 2.

assessment of future developments in axon targeting, such as combinations of these motifs, or the discovery of new ones.

The ability to characterize and compare motifs for axon targeting of exogenous genes *in vivo* has implications for the development of better tools to study the neurobiology of axons. Axon-targeting motifs have been effectively used to study the axonal anatomy of the nigro-striatal projection¹ and to explore the mechanisms of axon protection by the mutant Wld^S protein.¹² The ability to quantify the efficacy of different motifs in specific projections will enhance the utility of such approaches.

Our observations also have implications for the development of gene therapies that are intended to affect axon growth, integrity or function. The use of axon-targeting motifs may enhance effects at the axon level and diminish undesired off-target effects. For example, we have reported that constitutively active mutant forms of both the kinase Akt and the GTPase Rheb are capable of inducing axon re-growth in adult dopaminergic neurons.^{5,6} However, both of these mutants are potent oncogenes. Given that Akt and Rheb are likely to be signaling through the mammalian target of rapamycin kinase, and in view of evidence

that mammalian target of rapamycin signaling may occur locally in axons to regulate their growth,^{2,3} it may be possible to use axon-targeting motifs to direct these molecules to the axon, where the desired effects in axon growth are mediated, and thereby minimize expression in the cell body, where effects on cell proliferation are likely to occur. Although our future studies will be aimed at testing the potency of neuro-restorative effects in Parkinson's disease with these axonally targeted proteins, we believe our observations have potential use for therapy in other disorders where axonal loss is an early feature of disease such as in Alzheimer's disease and amyotrophic lateral sclerosis.¹⁷ In these disorders, axon-targeting motifs could be used not only to monitor the anatomy and early pathogenesis in the projection systems but also to direct proteins of interest to the distal axons to achieve a beneficial effect.

MATERIALS AND METHODS

Production of AAV vectors

To produce constructs incorporating axon-targeting sequences from β -actin, GAP-43 and APP, oligonucleotides were purchased from e-oligos

(Hawthorne, NY, USA). The axon-targeting sequence from tau was obtained by PCR amplification from rat cDNA. We used two control constructs. The first was the unmodified tdTomato-coding sequence. The second incorporated a dendritic-targeting sequence in the CamKII- α mRNA 3' UTR.¹⁸ This sequence was obtained by PCR amplification from rat cDNA. TdTomato-encoding plasmid was purchased from Addgene (Cambridge, MA, USA). All constructs were subcloned into an AAV2 backbone plasmid (pBL) that incorporated different regulatory elements. All nucleotide sequences in the AAV packaging constructs were confirmed before AAV production. AAVs were produced by the University of North Carolina Vector Core. The Vector Core uses a triple transfection protocol in suspension HEK293 cells and is purified by column chromatography. The formulation buffer is PBS with 5% sorbitol. All vectors used in this study were AAV1 serotype. The genomic titer of AAV-Tomato was 1×10^{12} viral genomes per ml, and those of AAV-Tomato-CaMKII- α , AAV-Tomato- β -actin- α , AAV-Tomato-Tau- α , AAV-GAPPal-Tomato and AAV-cAPP-Tomato were 5×10^{11} , 1×10^{12} , 2×10^{12} , 3×10^{12} and 2×10^{12} viral genomes per ml, respectively.

Intranasal AAV injection

Adult (8 week) male C57BL/6 mice were obtained from Charles River Laboratories, Wilmington, MA, USA. Mice were anesthetized with ketamine/xylazine solution and placed in a stereotaxic frame (Kopf Instruments, Tujunga, CA, USA) with a mouse adapter. The tip of a 5.0- μ l syringe needle (26S) was inserted to stereotaxic coordinates AP: -0.35 cm; ML: $+0.11$ cm; DV: -0.37 cm, relative to bregma. Viral vector suspension in a volume of 2.0 μ l was injected at 0.1 μ l min⁻¹ over 20 min.

Institutional review of animal protocols

All injection procedures, as described above, were approved by the Columbia University Institutional Animal Care and Use Committee.

Coronal sectioning and immunohistochemistry for Tomato

Mice were perfused through the left ventricle with 0.9% NaCl followed by 4.0% paraformaldehyde in 0.1 mol l⁻¹ phosphate buffer, pH 7.1. The brain was carefully removed and cut into midbrain and forebrain regions. The region containing the midbrain was postfixed for 1 week, cryoprotected in 20% sucrose overnight and then rapidly frozen by immersion in isopentane on dry ice. A complete set of serial sections was then cut through the substantia nigra (SN) at 30 μ m. Beginning with a random section between 1 and 4, every fourth section was processed. Sections were processed free-floating. The primary antibody was rabbit polyclonal to dsRed (Clontech, Mountain View, CA, USA) at 1:100. Sections were then treated with biotinylated protein A and avidin-biotinylated horseradish peroxidase complexes (ABC; Vector Labs, Burlingame, CA, USA). After immunoperoxidase staining, sections were thionin counterstained. The forebrain region containing the striatum was postfixed for 48 h, frozen without cryoprotection and processed as described above. We used immunoperoxidase staining for Tomato to quantify our results as the chromagen reaction product is stable under continued illumination making it suitable for stereology and striatal optical density measurements that require prolonged visualization of the tissue sections.

Stereology and striatal optical density measurements

The number of transduced neurons in the SN was determined by stereologic counts of tdTomato-positive profiles. The entire SN was identified as the region of interest. By use of the StereoInvestigator program (MicroBrightField, Williston, VT, USA), a fractionator probe was established for each section. The number of Tomato-positive neurons in each counting frame was determined by focusing down through the section, using $\times 100$ objective under oil, as required by the optical disector method. Our criterion for counting an individual neuron was the presence of its nucleus either within the counting frame, or touching the right or top frame lines (green), but not touching the left or bottom lines (red). The total number of Tomato-positive neurons for each side of the SN was then determined by the StereoInvestigator program. The optical density of striatal Tomato immunostaining was determined with an Analytical Imaging Station (Imaging Research, St Catharines, Ontario, Canada).

Quantitative morphologic analysis of Tomato-positive axons in the MFB

For this analysis, mice expressing GFP under the TH promoter¹⁹ were used. The SN was injected with AAV suspension as described above. Fifty-micrometer-thick horizontal sections were obtained and the section containing the A13 dopaminergic cell group, the third ventricle, the third ventricle recess and the MFB was chosen for further processing. A confocal microscope (Leica TCS SP5 AOBs, Exton, PA, USA) was used to obtain 20 optical planes through a 2- μ m vertical distance within the MFB. This z-stack was merged to form a maximal projection of the sampled volume. This procedure was performed in five adjacent fields (97 mm \times 97 mm) from medial to lateral across the MFB. The argon-ion laser with an excitation wavelength of 488 nm was used to visualize the GFP-positive dopaminergic axons and the helium-neon laser with an excitation wavelength of 543 nm was used to visualize the Tomato-positive axons in the MFB. The fields that were positive for GFP were selected for counting Tomato-positive axons. In order to count the number of Tomato axons passing in the rostro-caudal dimension through each sample volume, two lines were set crossing the maximal projection image at distance of 10.0 μ m apart. Every intact red axon crossing both lines was counted as positive.

Statistical analysis

Multiple comparisons among groups were performed by one-way analysis of variance and Tukey *post hoc* analysis. *N* indicates the number of animals used for each experiment. The condition that shows a statistically significant effect is indicated by the dotted line and the experimental condition that it is compared with is indicated by the solid line in each graph. All statistical analyses were performed using SigmaStat software (Systat Software, San Leandro, CA, USA).

CONFLICT OF INTEREST

The authors declare no conflict of interest.

ACKNOWLEDGEMENTS

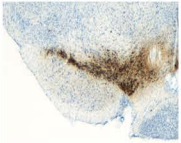
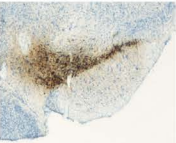
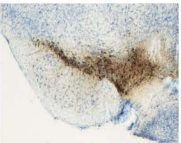
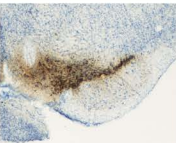
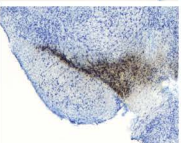
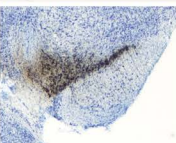
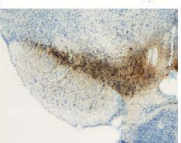
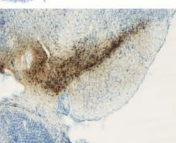
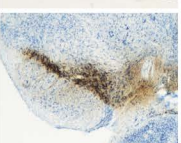
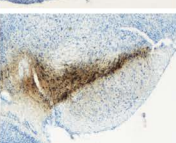
This work was supported by NIH NS38370, DOD W81XVH-12-1-0051, the Parkinson's Disease Foundation and the Parkinson Alliance (R.E.B.).

REFERENCES

- 1 Matsuda W, Furuta T, Nakamura KC, Hioki H, Fujiyama F, Arai R *et al*. Single nigrostriatal dopaminergic neurons form widely spread and highly dense axonal arborizations in the neostriatum. *J Neurosci* 2009; **29**: 444–453.
- 2 Lin AC, Holt CE. Function and regulation of local axonal translation. *Curr Opin Neurobiol* 2008; **18**: 60–68.
- 3 Campbell DS, Holt CE. Chemotropic responses of retinal growth cones mediated by rapid local protein synthesis and degradation. *Neuron* 2001; **32**: 1013–1026.
- 4 Wang W, van Niekerk E, Willis DE, Twiss JL. RNA transport and localized protein synthesis in neurological disorders and neural repair. *Dev Neurobiol* 2007; **67**: 1166–1182.
- 5 Kim SR, Chen X, Oo TF, Kareva T, Yarygina O, Wang C *et al*. Dopaminergic pathway reconstruction by Akt/Rheb-induced axon regeneration. *Ann Neurol* 2011; **70**: 110–120.
- 6 Kim SR, Kareva T, Yarygina O, Kholodilov N, Burke RE. AAV transduction of dopamine neurons with constitutively active Rheb protects from neurodegeneration and mediates axon regrowth. *Mol Ther* 2012; **20**: 275–286.
- 7 Kislauskis EH, Zhu X, Singer RH. Sequences responsible for intracellular localization of beta-actin messenger RNA also affect cell phenotype. *J Cell Biol* 1994; **127**: 441–451.
- 8 Zhang HL, Eom T, Oleynikov Y, Shenoy SM, Liebelt DA, Dichtenberg JB *et al*. Neurotrophin-induced transport of a beta-actin mRNA complex increases beta-actin levels and stimulates growth cone motility. *Neuron* 2001; **31**: 261–275.
- 9 Aronov S, Aranda G, Behar L, Ginzburg I. Axonal tau mRNA localization coincides with tau protein in living neuronal cells and depends on axonal targeting signal. *J Neurosci* 2001; **21**: 6577–6587.
- 10 El-Husseini Ael D, Craven SE, Brock SC, Bredt DS. Polarized targeting of peripheral membrane proteins in neurons. *J Biol Chem* 2001; **276**: 44984–44992.
- 11 Satpute-Krishnan P, DeGiorgis JA, Conley MP, Jang M, Bearer EL. A peptide zipcode sufficient for anterograde transport within amyloid precursor protein. *Proc Natl Acad Sci USA* 2006; **103**: 16532–16537.

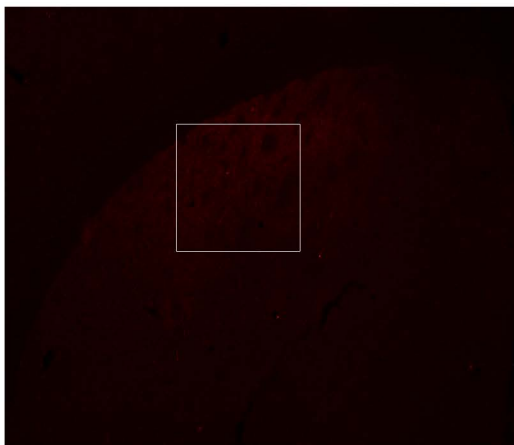
- 12 Babetto E, Beirowski B, Janeckova L, Brown R, Gilley J, Thomson D *et al*. Targeting NMNAT1 to axons and synapses transforms its neuroprotective potency *in vivo*. *J Neurosci* 2010; **30**: 13291–13304.
- 13 Biermann B, Ivankova-Susankova K, Bradaia A, Abdel Aziz S, Besseyrias V, Kapfhammer JP *et al*. The Sushi domains of GABAB receptors function as axonal targeting signals. *J Neurosci* 2010; **30**: 1385–1394.
- 14 Aranda-Abreu GE, Behar L, Chung S, Furneaux H, Ginzburg I. Embryonic lethal abnormal vision-like RNA-binding proteins regulate neurite outgrowth and tau expression in PC12 cells. *J Neurosci* 1999; **19**: 6907–6917.
- 15 Farina KL, Huttelmaier S, Musunuru K, Darnell R, Singer RH. Two ZBP1 KH domains facilitate beta-actin mRNA localization, granule formation, and cytoskeletal attachment. *J Cell Biol* 2003; **160**: 77–87.
- 16 Ross AF, Oleynikov Y, Kislauskis EH, Taneja KL, Singer RH. Characterization of a beta-actin mRNA zipcode-binding protein. *Mol Cell Biol* 1997; **17**: 2158–2165.
- 17 Schon EA, Przedborski S. Mitochondria: the next (neurode)generation. *Neuron* 2011; **70**: 1033–1053.
- 18 Blichenberg A, Rehbein M, Muller R, Garner CC, Richter D, Kindler S. Identification of a cis-acting dendritic targeting element in the mRNA encoding the alpha subunit of Ca²⁺/calmodulin-dependent protein kinase II. *Eur J Neurosci* 2001; **13**: 1881–1888.
- 19 Sawamoto K, Nakao N, Kobayashi K, Matsushita N, Takahashi H, Kakishita K *et al*. Visualization, direct isolation, and transplantation of midbrain dopaminergic neurons. *Proc Natl Acad Sci USA* 2001; **98**: 6423–6428.

Supplementary Information accompanies this paper on Gene Therapy website (<http://www.nature.com/gt>)

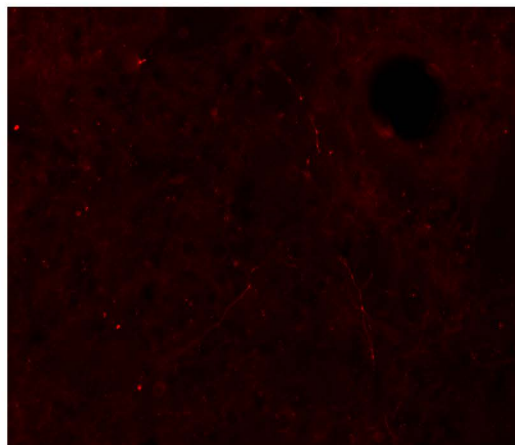
	Control	Injected
Tomato		
Tomato-CaMKII-zip		
Tomato-Tau-zip		
GAPpal-Tomato		
cAPP-Tomato		

TOMATO β -ACTIN-ZIP

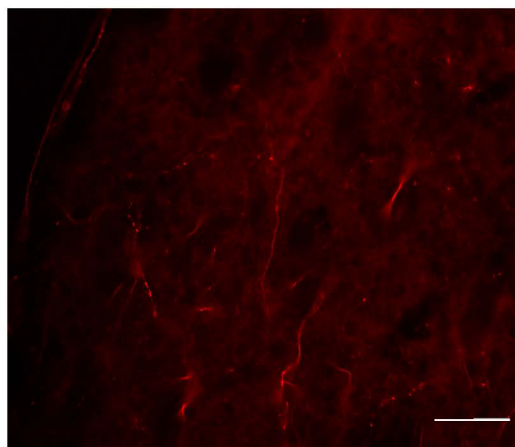
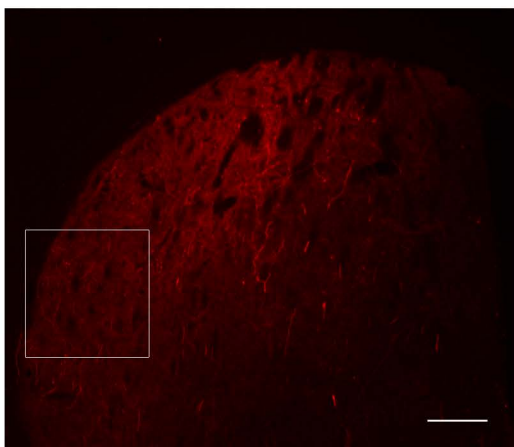
4X: Scale 100 μ m

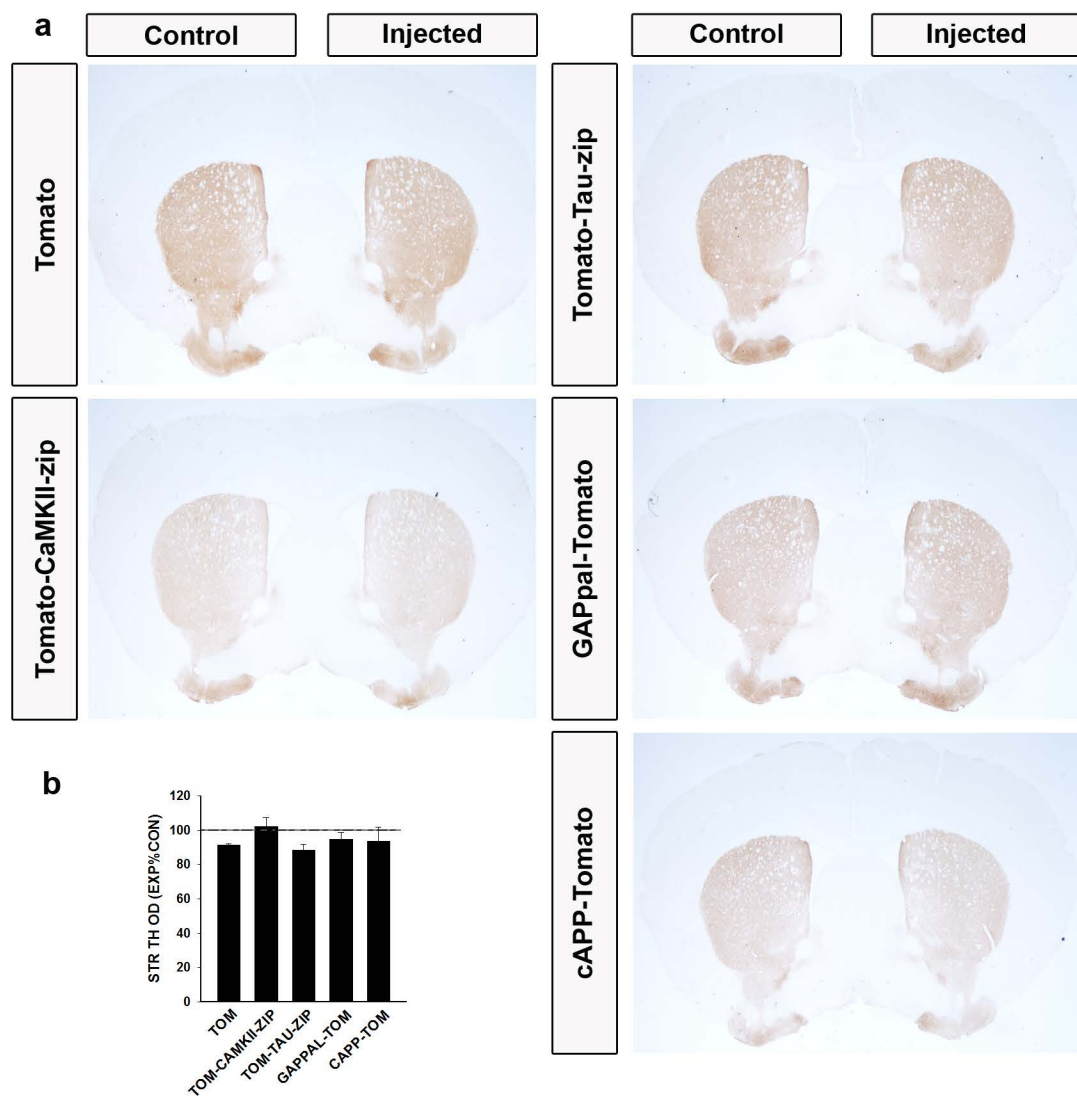


10X: Scale 50 μ m



TOMATO-TAU-ZIP





Supplementary Figure 1: Effect of the different control and axon targeting viral vectors on dopamine neurons in the SNpc

Coronal sections through the SN were processed for TH immunoperoxidase staining with thionin counterstain at 4 weeks following intra-nigral injection of the different control and axon targeting viral vectors. Representative sections from the SN reveal no toxicity to the TH positive neurons on the injected side as compared to the control side.

Supplementary Figure 2: A comparison between the two axon targeting mRNA zipcodes

Mice were injected with either Tomato- β -actin-zip or Tomato-tau-zip in the SN and 4 weeks later coronal sections of the striatum were observed under an epifluorescence microscope. Greater Tomato fluorescence in the striatum would indicate better axon targeting capability of the construct. The mRNA zipcode in tau results in a much higher Tomato fluorescence in the striatum when compared to the mRNA zipcode in β -actin. White boxes in the panels to the left delineate the regions indicated at a higher power in the panels to the right. The higher power images show greater number of fibers in the striatum and higher Tomato fluorescence indicating stronger delivery of Tomato to the terminal fields with the Tomato-tau-zip construct.

Supplementary Figure 3: Assessment of striatal TH toxicity with the controls and axon targeting viral vectors

(a) Coronal sections through the striatum were processed for TH immunoperoxidase staining at 4 weeks following intra-nigral injection of the different control and axon targeting viral vectors. (b) Optical density of TH in the striatum was measured and the value of striatal TH optical density on the injected side was expressed as a percentage of the control un-injected side. The graph indicates no toxicity to the dopaminergic terminals in the striatum with the different viral vectors.